Electronic Supplementary Material (ESI) for ChemComm.

Supporting Information to

The metalation of hen egg white lysozyme impacts protein stability as shown by ion mobility mass spectrometry, differential scanning calorimetry, and X-ray crystallography

Matthew P. Sullivan,[ab] Michael Groessl,[c] Samuel M. Meier,[d] Richard L. Kingston,[b] David C. Goldstone,[b] and Christian G. Hartinger*[a]

[a] *School of Chemical Sciences, University of Auckland, Private Bag 92019, Auckland 1142, New Zealand.*

[b] *School of Biological Sciences, University of Auckland, Private Bag 92019, Auckland 1142, New Zealand.*

[c] *TOFWERK, Uttigenstr. 22, 3600 Thun, Switzerland.*

[d] *Institute of Analytical Chemistry, University of Vienna, Waehringer Str. 38, A-1090, Vienna, Austria.*

Table of Contents

Additional figures highlighting the metal binding sites on HEWL

Crystal data, collection, phasing and refinement

Experimental procedures

References

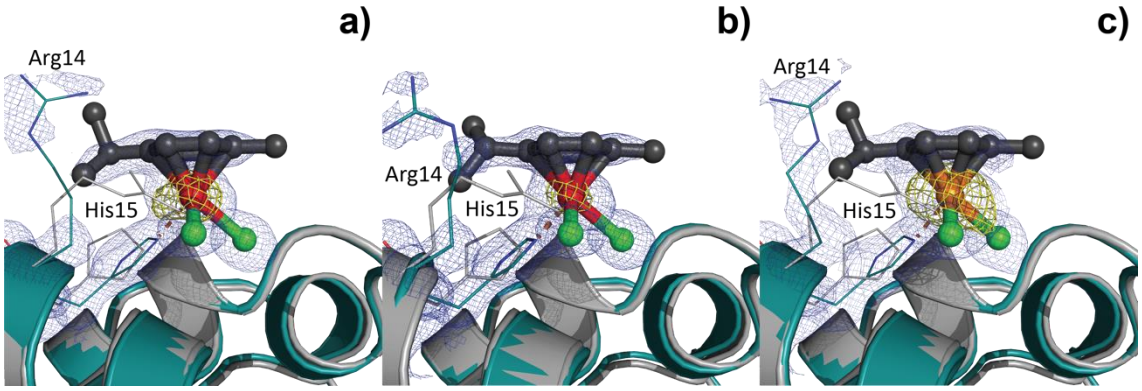

Figure S1. Ru and Os binding sites overlaid with the native structure of HEWL (PDB ID 4NHI) shown in grey, highlighting the position changes of residues Arg14 and His15, as results from the reaction between HEWL and **1a** (a), **1b** (b) and **2** (c).

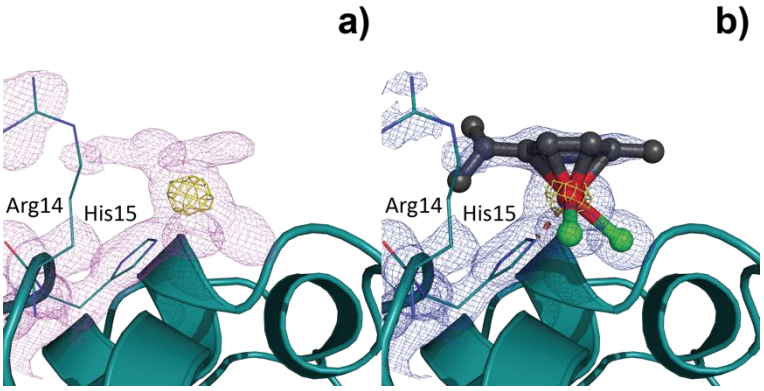

Figure S2. Crystal structure of the adduct formed between **1b** and HEWL. a) Binding site I, showing the unbiased electron density (magenta) contoured to 1σ and the anomalous difference map (yellow) contoured to 4σ. b) Placement of Ru(cym)Cl_2 with the refined electron density map (blue) around the ligand contoured to 1σ with anomalous difference map. Ligand atom colors: Carbon (dark grey), Ruthenium (red), Bromido (dark green)

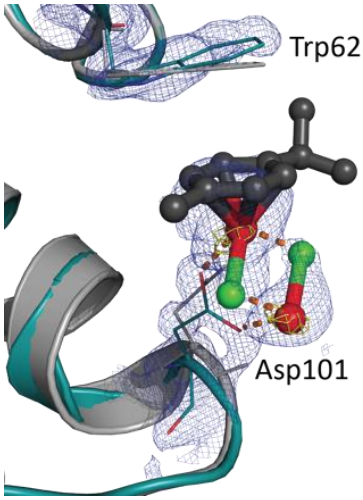

Figure S3. (cym)Ru(μ-Cl_2)Ru binding site (site II) overlaid with the native structure (PDB ID 4NHI) shown in grey, highlighting the position changes of residues Asp101 and Trp62.

To further support the positioning of the organometallic moieties, maps were generated using phenix.polder,[1] which allow for weak ligand density to be viewed in sharper detail (Figs. S4 and S5), and composite omit maps[2] with simulated annealing further proved the ligand identity (Figs. S6 and S7).

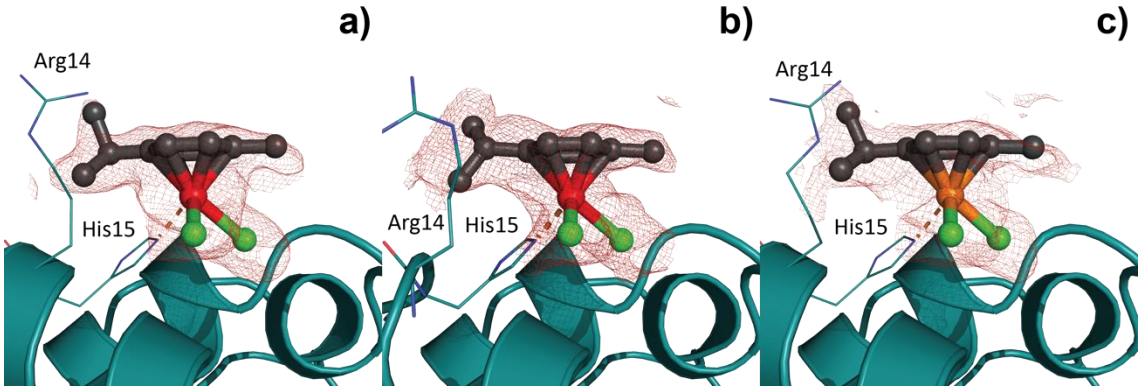

Figure S4. Ru/Os binding site with a map generated by phenix.polder contoured to 1σ with M(cym)Cl_2 (**1a**, a; **1b**, b; **2**, c) excluded which allows for ligand densities to be displayed with the exclusion of bulk solvent. The residues Arg14 and His15 are shown as a reference.

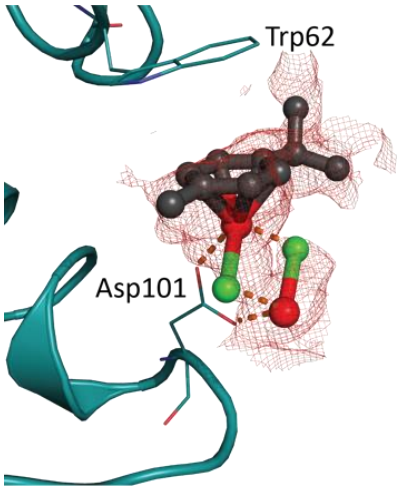

Figure S5. Ru binding site (site II) found for **1a** with a map generated with phenix.polder contoured to 0.7σ with (cym)Ru(μ-Cl_2)Ru excluded which allows for ligand densities to be displayed with the exclusion of bulk solvent. The residues Asp101 and Trp62 are shown as a reference.

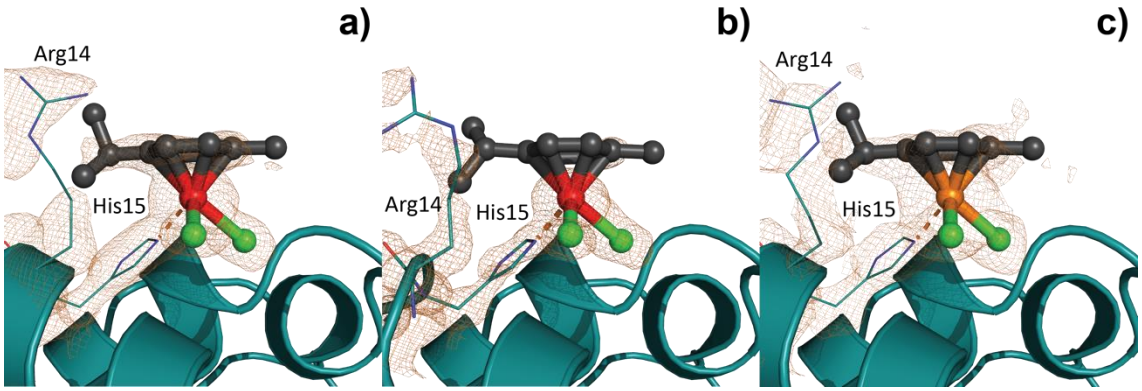

Figure S6. Ru/Os binding sites with composite omit maps with simulated annealing displaying the fitting of M(cym)Cl_2 for the reactions between HEWL and **1a** (a), **1b** (b) and **2** (c).

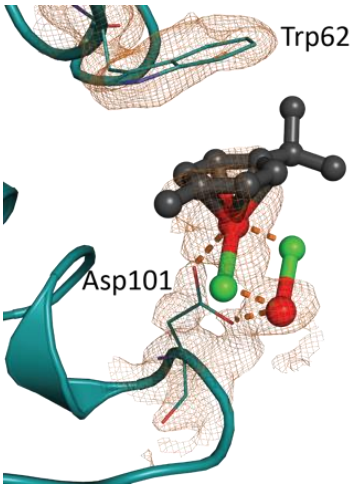

Figure S7. Binding site II found for **1a** with a composite omit map with simulated annealing displaying the fitting of (cym)Ru(μ-Cl_2)Ru and the positioning of Trp62 and Asp101.

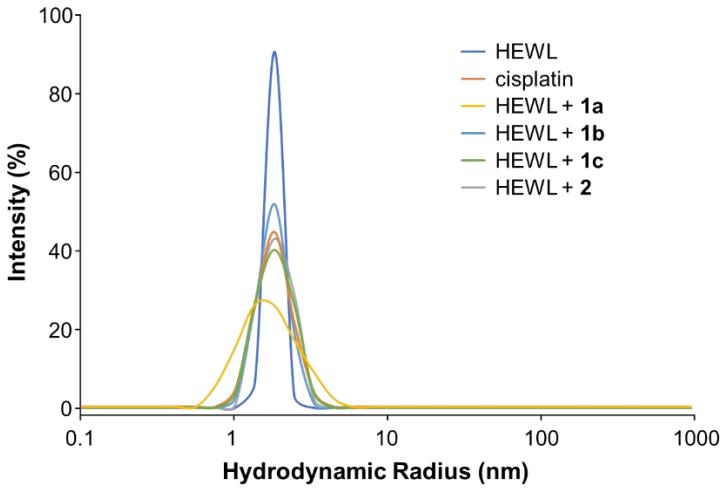

Figure S8. Dynamic light scattering analysis revealed an increase in heterogeneity/polydispersity but no change in average protein hydrodynamic radius. The intensity distributions were computed using the regularization procedure within the programme Dynamics (Wyatt Technology).

Experimental

Protein crystallography

HEWL crystals of 0.1–0.2 mm were grown from a reservoir solution consisting of NaCl (0.8 M) and sodium acetate (0.1 M) at pH 4.7 which was mixed with an equal volume of HEWL (100 mg/ml).[3] The resultant crystals formed within 24 h, and were then transferred into a drop of reservoir solution supplemented with **1a** (0.89 mg, 2 mg/mL), **1b** (1.28 mg, 2 mg/mL), **1c** (1.54 mg, 2 mg/mL) or **2** (1.32 mg, 2 mg/mL). After a period of 24 h, the crystals turned yellow and were transferred into a cryoprotectant of 20% glycerol, NaCl (0.8 M) and Na acetate (0.1 M) at pH 4.7, and flash frozen in liquid nitrogen.

Data collection and analysis

X-ray diffraction data were collected on the crystallography beamlines MX1 and MX2 at the Australian Synchrotron.[4] Data were processed with either XDS[5] or MOSFLM.[6] The protein crystallised in the space group $P4_32_12$. The structures were determined by molecular replacement using a monomer of lysozyme (PDB ID 4NHI) as a search model in PHASER.[7] The models were refined with iterative rounds of refinement and model building in REFMAC[8] and COOT.[9] Sodium ion placement was aided by the use of the WASP server at USF.[10] The anomalous difference maps were generated using FFT.[11] The Ru- or Os-containing compounds were reformatted using Gaussian[12] (from their molecular structures), while the final PDB and CIF files were generated by phenix.elbow.[13]

Table S1. Crystal data, collection, phasing and refinement.

	1a	**1b**	**2**
PDB ID	5V4G	5V4H	5V4I
Data collection	AS MX1	AS MX2	AS MX2
Space group	$P4_32_12$	$P4_32_12$	$P4_32_12$
Cell dimensions a, b, c (Å) α, β, γ (∘)	a = b = 80.3, c = 36.9 90.0, 90.0, 90.0	a = b = 80.4, c = 36.6 90.0, 90.0, 90.0	a = b = 80.6, c = 37.0 90.0, 90.0, 90.0
Wavelength (Å)	0.9537	0.9537	0.9537
Unique reflections	38333	32718	20117
Resolution range (Å)*	40.14-1.20 (1.22-1.20)	47.70-1.22 (1.24-1.22)	40.30-1.50 (1.53-1.50)
Rpim (%)*	0.02 (0.74)	0.04 (0.78)	0.05 (0.29)
I/σ(I)*	16.2 (1.1)	8.4 (1.0)	11.0 (2.5)
CC(1/2)*	0.999 (0.362)	0.995 (0.433)	0.996 (0.775)
Completeness (%)*	99.9 (98.9)	91.8 (91.6)	100.0 (100.0)
Multiplicity*	14.0 (11.0)	5.1 (5.0)	9.2 (7.6)
Phasing (MR Phaser)			
LLG	3460	3685	1975
Z-score	55.5	58.7	42.3
Refinement			
Resolution (Å)	40.14-1.20	47.70-1.22	36.04-1.50
Rwork/Rfree (%)	0.18/0.21	0.15/0.19	0.23/0.28
No. atoms (residues)			
Protein	1047 (129)	1051 (129)	1038 (129)
Water	104	99	71
Sodium	1	1	1
Ligands - site I	13 (1)	13 (1)	13 (1)
- site II	12 (1)/2 (1)	-	-
B-factors (Å^2)			
Wilson	11.6	11.2	9.0
Protein	17.6	17.4	18.8
Water	25.7	24.4	26.6
Ligand - site I	26.5 (0.9 occupancy)	25.6 (0.8 occupancy)	28.8 (0.9 occupancy)
site II	32.4 (0.5 occupancy)/ 42.2 (0.5 occupancy)	-	-
R.M.S. deviations			
Bond lengths (Å)	0.009	0.010	0.009
Bond angles (∘)	1.49	1.45	1.33

* Data for outer shell are shown in parentheses.

Ion mobility -mass spectrometry

All IM-MS measurements were carried out on a Tofwerk IMS-TOF (Thun, Switzerland). The system comprises an ESI source, a 10 cm desolvation tube, a 20 cm drift tube (both made from resistive glass) and a Tofwerk HTOF (TOF-MS) with two-stage interface to the IMS. Desolvation and drift tubes were thermostated at 50 °C with nitrogen as the buffer gas. Ion mobility separation was carried out at a field strength of ca. 400 V/cm (reduced electric field strength ca. 2 Td). Drift-tube pressure was set to 1000 mbar. Samples were introduced directly into the ESI source at 1 µl/min. The instrument was operated from m/z 400 to 3000 in both positive ion mode. The mass spectrometer was calibrated externally using a mixture of tetraalkylammonium salts and Ultramark 1621. Raw IMS-TOF data was post-processed using Tofware (Tofwerk, Switzerland). Samples were prepared in pure water and incubated for up to 96 h at a metallodrug : protein ratio from 2 : 1 to 10 : 1 (protein concentration fixed at 10 uM).

Collision cross section measurements

Measured ion mobility drift times have to be corrected for time spent outside the drift tube (i.e., the interface region of the mass spectrometer) for precise determination of collision cross sections (CCS). Corrected drift times are determined from a plot of the measured drift time versus the inverse drift voltage. Drift time measurements were carried out at five different drift potentials (from 8 to 12 kV) and the y-intercept of the plot vs. 1/field strength (the “non-mobility” component of the drift time) subtracted from the measured drift time to obtain the corrected drift time. CCS can then be directly calculated from the corrected drift times, and no external calibration is needed. A modified zero-field equation, called the momentum transfer scan law, was used to correct for field-dependent momentum transfer and collision frequency. Corrected drift times and CCS are determined automatically by the post processing software (Tofware). The integrated collision cross sections can be calculated using equation S1.

$$\Omega = \frac{3}{16}\left(\frac{2\pi}{\mu k T}\right)^{1/2}\frac{qzE}{v_d N}\left[1+\left(\frac{\beta_{MT}}{\alpha_{MT}}\right)^2\left(\frac{v_d}{v_T}\right)^2\right]^{-1/2} \quad \text{eq. S1}$$

Ω = integrated collision cross section
μ = reduced mass of the analyte and the drift gas
k = Boltzmann's constant
T = temperature of the drift cell
q= elementary charge
z = charge number
E = electric field
v_d = drift velocity
N = neutral gas number density
β_{MT} = correction coefficient for momentum transfer
α_{MT} = correction coefficient for collision frequency
v_T = thermal velocity

Table S2. Relative IMS peak areas (%) for HEWL and its adducts with **1a** at 9+ and 10+ charge states.

Charge State	Peak Identification	Compact Conformer (%) *	Expanded Conformer (%) *
7+	HEWL	100	0
	Monoadduct	100	0
	Bisadduct	100	0
9+	HEWL	52	48
	Monoadduct	62	38
	Bisadduct	73	27
10+	HEWL	28	72
	Monoadduct	40	60
	Bisadduct	43	57

* relative standard deviation = ~3%; n = 3.

Differential Scanning Calorimetry

The metal compounds were incubated with HEWL (1.4 mM) at molar ratios of 2 : 1 (**1a**) or 1 : 1 (**1b**, **1c**, **2**) in sodium phosphate buffer (100 mM, pH 7.3) for 1 week. DSC measurements (20 to 95 °C) were made on these solutions using a TA instruments Nano DSC system equipped with an

autosampler, with the buffered metal compounds in the reference cell. All solutions were outgassed before measurement and a scan rate of 2 °C/min was employed.

Dynamic Light Scattering

The metal compounds were incubated with HEWL (1.4 mM) at molar ratios of 2 : 1 (**1a**) or 1 : 1 (**1b**, **1c**, **2**) in sodium phosphate buffer (100 mM, pH 7.3) for 1 week. The DLS measurements (200 acquisitions for each sample) were made using a Wyatt Dynapro Titan dynamic light scattering instrument. All solutions were outgassed and centrifuged before measurement.

References

1. D. Liebschner, P. V. Afonine, N. W. Moriarty, B. K. Poon, O. V. Sobolev, T. C. Terwilliger and P. D. Adams, *Acta Crystallogr. D Biol. Crystallogr.*, 2017, **73**, 148-157.
2. T. C. Terwilliger, R. W. Grosse-Kunstleve, P. V. Afonine, N. W. Moriarty, P. D. Adams, R. J. Read, P. H. Zwart and L. W. Hung, *Acta Crystallogr. D Biol. Crystallogr.*, 2008, **64**, 515-524.
3. C. C. F. Blake, R. H. Fenn, L. N. Johnson, D. F. Koenig, G. A. Mair, A. C. T. North, J. W. H. Oldham, D. C. Phillips, R. J. Poljak, V. R. Sarma and C. A. Vernon, *How the structure of lysozyme was actually determined*, 2006.
4. N. P. Cowieson, D. Aragao, M. Clift, D. J. Ericsson, C. Gee, S. J. Harrop, N. Mudie, S. Panjikar, J. R. Price, A. Riboldi-Tunnicliffe, R. Williamson and T. Caradoc-Davies, *J. Synchrotron Radiat.*, 2015, **22**, 187-190.
5. W. Kabsch, *Acta Crystallogr. D Biol. Crystallogr.*, 2010, **66**, 133-144.
6. T. G. Battye, L. Kontogiannis, O. Johnson, H. R. Powell and A. G. Leslie, *Acta Crystallogr. D Biol. Crystallogr.*, 2011, **67**, 271-281.
7. A. J. McCoy, R. W. Grosse-Kunstleve, P. D. Adams, M. D. Winn, L. C. Storoni and R. J. Read, *J. Appl. Crystallogr.*, 2007, **40**, 658-674.
8. G. N. Murshudov, A. A. Vagin and E. J. Dodson, *Acta Crystallogr. D Biol. Crystallogr.*, 1997, **53**, 240-255.
9. P. Emsley and K. Cowtan, *Acta Crystallogr. D Biol. Crystallogr.*, 2004, **60**, 2126-2132.
10. M. Nayal and E. Di Cera, *J. Mol. Biol.*, 1996, **256**, 228-234.
11. R. J. Read and A. J. Schierbeek, *J. Appl. Crystallogr.*, 1988, **21**, 490-495.
12. M. J. Frisch, G. W. Trucks, H. B. Schlegel, G. E. Scuseria, M. A. Robb, J. R. Cheeseman, G. Scalmani, V. Barone, B. Mennucci, G. A. Petersson, H. Nakatsuji, M. Caricato, X. Li, H. P. Hratchian, A. F. Izmaylov, J. Bloino, G. Zheng, J. L. Sonnenberg, M. Hada, M. Ehara, K. Toyota, R. Fukuda, J. Hasegawa, M. Ishida, T. Nakajima, Y. Honda, O. Kitao, H. Nakai, T. Vreven, J. A. Montgomery, J. E. Peralta, F. Ogliaro, M. Bearpark, J. J. Heyd, E. Brothers, K. N. Kudin, V. N. Staroverov, R. Kobayashi, J. Normand, K. Raghavachari, A. Rendell, J. C. Burant, S. S. Iyengar, J. Tomasi, M. Cossi, N. Rega, J. M. Millam, M. Klene, J. E. Knox, J. B. Cross, V. Bakken, C. Adamo, J. Jaramillo, R. Gomperts, R. E. Stratmann, O. Yazyev, A. J.

Austin, R. Cammi, C. Pomelli, J. W. Ochterski, R. L. Martin, K. Morokuma, V. G. Zakrzewski, G. A. Voth, P. Salvador, J. J. Dannenberg, S. Dapprich, A. D. Daniels, Farkas, J. B. Foresman, J. V. Ortiz, J. Cioslowski and D. J. Fox, (Gaussian 09, Revision B.01); 2009.

13. N. W. Moriarty, R. W. Grosse-Kunstleve and P. D. Adams, *Acta Crystallogr. D Biol. Crystallogr.*, 2009, **65**, 1074-1080.